the stimulating rivalry between theory and experiment.

It is also of interest to compare our result with X-ray crystallographic studies of solid silaethylenes stable at room temperature. The initial X-ray study, by Brook and co-workers,[4] was of the highly substituted sila enol ether, $(Me_3Si)_2Si{=}C(OSiMe_3)$(1-adamantyl). It gave a "long" Si=C distance of 1.764 (3) Å. However, the bulky 1-adamantyl substituent noticeably twists the double bond, by 14.6°, and thereby lengthens it.[1] More recently an X-ray structure has been determined by Müller's group[5] for $Me_2Si{=}C(SiMe_3)(SiMe\text{-}t\text{-}Bu_2)$ in which the substituents are less bulky and less polar, giving a twist about the Si=C bond of only 1.6°. In it, the Si=C bond length of 1.702 (5) Å is substantially shorter. However, it is still definitely longer than the value of 1.692 (3) Å found for DMSE in the gas phase.

The small angle found for ∠(C—Si—C) merits discussion. It comes largely from fitting the internal rotation fine structure, which gives $2\theta = 111.2\ (2)°$, and from the "large" experimental value for the *B* rotational constant. In principle, a larger ∠(C—Si—C) could be obtained by forcing a large negative methyl group tilt on the fit, decreasing r_o(Si=C) and increasing r_o(C—Si). However, both the theoretical structure and the fitting of the DMSE rotational constants give a tilt of only about −0.1°.

The magnitude of the tilt is a measure of the extent to which the inherent C_{3v} symmetry of a methyl group is perturbed in compounds where it is attached to a less symmetric group.[21,26] In isobutylene, methyl group tilt of 0.8 (2)° was found.[15] In DMSE, the methyl groups are farther apart and have only half as large a barrier to internal rotation, so one would expect smaller tilt in it. Indeed this is the case for propane and its silicon analogue. In propane, there apparently is tilt of the methyl groups by 0.8° toward the CH_2 group,[27] while in $(CH_3)_2SiH_2$ the value of 2θ is the same (111°) as ∠(C–Si–C) from the inertial analysis.[17] Such arguments lead us to prefer the effective structure presented in Table III.

Acknowledgment. We thank C. E. Dykstra and L. K. Montgomery for encouraging and helpful discussions and T. C. Germann for doing some of the fitting. We are indebted to R. H. Schwendeman for giving us his STRFTQ program and to D. H. Sutter for the KC3IAM program. Our work was supported by NSF under Grants DMR-86-12860 and -89-20538 and CHE-85-20519 and -88-20359. Also, acknowledgment is made to the donors of the Petroleum Research Fund, administered by the American Chemical Society, for partial support of this research.

(26) Flood, E.; Pulay, P.; Boggs, J. E. *J. Am. Chem. Soc.* **1977**, *99*, 5570.
(27) Hirota, E.; Matsumara, C.; Morino, Y. *Bull. Chem. Soc. Jpn.* **1967**, *40*, 1124.

Electronic Structures of Trifluoro-, Tricyano-, and Trinitromethane and Their Conjugate Bases

Jerzy Cioslowski,* Stacey T. Mixon, and Eugene D. Fleischmann

Contribution from the Department of Chemistry and Supercomputer Computations Research Institute, Florida State University, Tallahassee, Florida 32306-3006. *Received July 11, 1990*

Abstract: The electronic structures of CHF_3, $CH(CN)_3$, and $CH(NO_2)_3$ and their conjugate bases are studied at the HF/6-31G* and HF/6-31++G** levels of theory. Topological features of the electron densities in the systems under study are interpreted within the framework of Bader's theory of atoms in molecules. The observed changes in geometry, the electron densities at the critical points, and the GAPT charges reveal the presence of Y-aromaticity in the $C(CN)_3^-$ and $C(NO_2)_3^-$ anions. Unusual weak bonds between the oxygen atoms belonging to different nitro groups in the $C(NO_2)_3^-$ anion are found. Absolute gas-phase acidities (proton affinities of the conjugate bases) are computed. There is no correlation between the acidities and any of the following molecular indices: the length and the stretching force constant of the C–H bond, the topological parameters of the C–H bond point, the Bader and GAPT atomic charges of the hydrogen atoms in the neutral molecules or of the carbon atoms in either neutral molecules or the corresponding anions. The GAPT charges appear to provide a better description of the electron density redistribution upon deprotonation than the Bader ones.

Introduction

Although methane is itself an extremely weak acid, some of its substituted derivatives have acidity comparable to that of inorganic acids. In particular, tricyanomethane (cyanoform) and trinitromethane (nitroform) form salts that are stable in water.[1] The extraordinary stability of the tricyanomethanide (cyanoformide) and trinitromethanide (nitroformide) anions is due to resonance effects. In contrast, the increased acidity of trifluoromethane (fluoroform) arises from the electron-withdrawing character of the fluorine substituent.

The modern quantum-mechanical calculations fare reasonably well in predicting both the gas-phase and in-solvent acidities. Accurate calculations of the absolute gas-phase acidities have become feasible after introduction by Chandrasekhar et al.[2] of Gaussian basis sets augmented by diffuse functions. Subsequently, proton affinities of several systems were studied, including, for example, the $CH_{n-1}X_{4-n}^-$ (n = 1–4, X = F, CN, NO_2)[3] and the XH_3^- (X = C, N, O, F, Si, P, S, and Cl)[4] series of anions. Monte Carlo simulations utilizing ab initio generated information about molecular structures and potentials were used to calculate the acidities of several organic acids in water.[5]

Despite the important role they play in organic chemistry, relatively little is known about the electronic structures of cyanoform and nitroform and their conjugate bases. In fact, even the gas-phase geometries of $CH(CN)_3$[6] and $CH(NO_2)_3$[7] are known

(1) Pearson, R. G.; Dillon, R. C. *J. Am. Chem. Soc.* **1953**, *75*, 2439. Boyd, R. H. *J. Chem. Phys.* **1963**, *67*, 737.
(2) Chandrasekhar, J.; Andrade, J. G.; Schleyer, P. v. R. *J. Am. Chem. Soc.* **1981**, *103*, 5609, 5612. Clark, T.; Chandrasekhar, J.; Spitznagel, G. W.; Schleyer, P. v. R. *J. Comput. Chem.* **1983**, *4*, 294.
(3) Edgecombe, K. E.; Boyd, R. J. *Can. J. Chem.* **1983**, *61*, 45. Edgecombe, K. E.; Boyd, R. J. *Can. J. Chem.* **1984**, *62*, 2887.
(4) Gordon, M. S.; Davis, L. P.; Burggraf, L. W.; Damrauer, R. *J. Am. Chem. Soc.* **1986**, *108*, 7889.
(5) Gao, J.; Garner, D. S.; Jorgenser, W. L. *J. Am. Chem. Soc.* **1986**, *108*, 4784. Jorgensen, W. L.; Briggs, J. M. *J. Am. Chem. Soc.* **1989**, *111*, 4190.
(6) Bak, B.; Svanholt, H. *J. Mol. Struct.* **1977**, *37*, 153.
(7) Sadova, N. I.; Popik, N. I.; Vilkov, L. V.; Pankrushev, J. A.; Shlyapochnikov, V. A. *J. Chem. Soc., Chem. Commun.* **1973**, 708.

0002-7863/91/1513-4751$02.50/0

Table I. Calculated Total Energies and Dipole Moments of CHX_3 and CX_3^-[a]

X	CHX_3 E_{HF}	CHX_3 μ_{HF}	CX_3^- E_{HF}
F	−336.771 64	1.6984	−336.117 58
	(−336.787 78)	(1.8680)	(−336.160 00)
CN	−315.346 87	2.9500	−314.846 94
	(−315.355 87)	(3.0059)	(−314.863 66)
NO_2	−650.539 11	2.5529	−650.027 52
	(−650.561 57)	(2.5488)	(−650.056 02)

[a] All values are at the HF/6-31G* geometries. Values are at the HF/6-31++G** level in parentheses. Total energies in au and dipole moments in D.

only with a very limited accuracy and their gas-phase acidities have never been measured. The previously reported quantum-mechanical calculations[3] were carried out with rather small basis sets, although some discussion on the basis set dependence of the calculated geometries and proton affinities was undertaken.

In this paper we report results of detailed electronic structure calculations on the CHX_3 molecules and the CX_3^- anions (X = F, CN, NO_2). The optimized geometries, gas-phase acidities, and dipole moments are calculated at the HF/6-31G* and the HF/6-31++G** levels of theory. The computed molecular wave functions are interpreted with the help of Bader's theory of atoms in molecules[8-11] and the GAPT population analysis.[12-17] The resulting molecular indices, such as, for instance, atomic charges and electron densities at the critical points, allow us to draw conclusions about the different factors that contribute to the unusually high acidities of these molecules.

Computational Techniques

The geometry optimizations were carried out at the HF/6-31G* level[18] with the GAUSSIAN 88 suite of codes,[19] running on the VAXstation 3540. All vibrational frequencies were calculated at the same level of theory. In addition, HF/6-31++G*[2] energies were computed at the HF/6-31G* optimized geometries.

The electron density was analyzed within the topological theory of atoms in molecules.[8-11] It has been shown repeatedly that the electron density, ρ, can be used to define molecular structures, to characterize atomic interactions, and to identify reactive sites in molecules. Some atoms are connected by gradient paths originating at the respective nuclei and terminating at a common critical point, where $\vec{\nabla}\rho = 0$. If this critical point is found to be a minimum in ρ along the path linking the atoms and a maximum in the other two orthogonal directions, then the paths are called bond paths and the common critical point is called a bond point. The set of all bond paths in a molecule provides a topological definition of molecular structure by indicating the major interactions between atoms.[8] Characterization of these interactions is aided by calculating values of $\rho(\vec{r})$ and $\nabla^2\rho(\vec{r})$ at the bond point, denoted ρ_{crit} and $\nabla^2\rho_{crit}$. For example, there are known relations between the bond order and the value of ρ_{crit}.[9] In addition, the value of $\nabla^2\rho_{crit}$ can serve as an indicator of the bond type.[10] Positive values are found for closed shell interactions, as in ionic and hydrogen bonds. Negative values are characteristic of shared interactions, as in covalent bonds. Finally, atomic properties, such as atomic charges, are obtained in the topological method by integration over the atomic basins that are traced out by all the paths of steepest descent in the electron density originating from the nuclei in question.[11] The properties of atoms and bonds reported in this paper were calculated with the EXTREM and PROAIM programs of Bader et al.[11]

The recently developed GAPT partitioning method[12-17] was also used to calculate effective atomic charges. The GAPT charges, which are computed from the derivatives of the molecular dipole moments with respect to the Cartesian coordinates of the nuclei in question,[12] have been found to provide a good representation of the electron distribution in such diverse systems as complexes of borabenzene with N_2 and CO,[13] inorganic complexes of transition metals,[14] various organic molecules and transition states,[15] two isomers of the $Li_2C_2O_2$ molecule,[16] and the atoms and ions trapped inside the C_{60} cage ("footballene").[17]

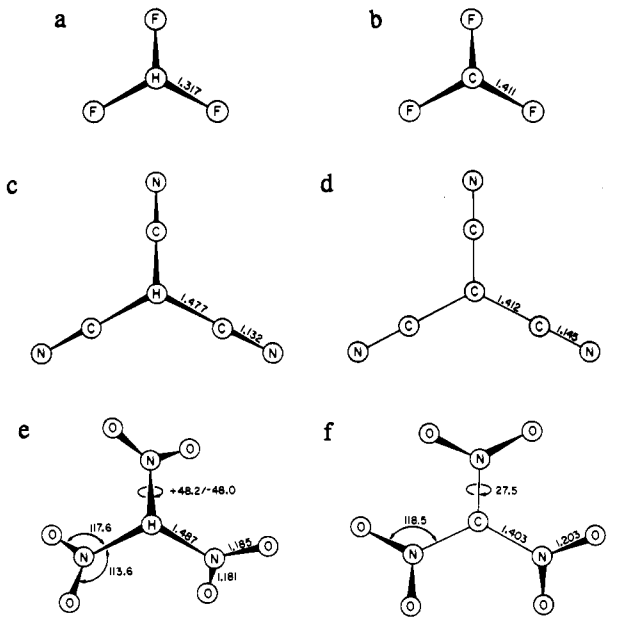

Figure 1. The HF/6-31G* optimized geometries as seen along the C_3 symmetry axes (note that in the CHX_3 molecules the carbon atoms lie directly under the hydrogens): (a) CHF_3, (b) CF_3^-, (c) $CH(CN)_3$, (d) $C(CN)_3^-$, (e) $CH(NO_2)_3$, (f) $C(NO_2)_3^-$.

Table II. Calculated Bond Angles between the C–X Bonds and the Molecular Symmetry Axes in CHX_3 and CX_3^- and the C–H Bond Lengths and Force Constants in CHX_3[a]

X	α CHX_3	α CX_3^-	R_{C-H}	κ_{C-H}
F	110.4	118.2	1.0741	0.4082
CN	107.8	90.0	1.0853	0.3741
NO_2	109.2	90.0	1.0727	0.4107

[a] At the HF/6-31G* level.

Results and Discussion

The calculated total energies for each species studied are listed in Table I, along with the corresponding dipole moments for the neutral molecules. The calculated dipole moment of CHF_3 (1.87 D) is in semiquantitative agreement with the experimental value of 1.65 D.[20]

The HF/6-31G* optimized geometries of all molecules studied are shown in Figure 1a–f. The vibrational frequency calculations prove that all of these stationary points are true (and very likely global) minima on the respective potential energy hypersurfaces as characterized by all positive eigenvalues of the energy Hessian. In addition, the calculated bond angles between the C–X bonds (X = F, CN, NO_2) and the molecular symmetry axes are listed for CHX_3 and CX_3^- in Table II together with the C–H bond

(8) Bader, R. F. W.; Nguyen-Dang, T. T.; Tal, Y. *Rep. Prog. Phys.* **1981**, *44*, 893. Bader, R. F. W.; Nguyen-Dang, T. T. *Adv. Quantum Chem.* **1981**, *14*, 63.
(9) Bader, R. F. W.; Slee, T. S.; Cremer, D.; Kraka, E. *J. Am. Chem. Soc.* **1983**, *105*, 5061.
(10) Bader, R. F. W.; Essen, H. *J. Chem. Phys.* **1984**, *80*, 1943.
(11) Biegler-Konig, F. W.; Bader, R. F. W.; Tang, T. H. *J. Comput. Chem.* **1982**, *3*, 317.
(12) Cioslowski, J. *J. Am. Chem. Soc.* **1989**, *111*, 8333.
(13) Cioslowski, J.; Hay, P. J. *J. Am. Chem. Soc.* **1990**, *112*, 1707.
(14) Cioslowski, J.; Hay, P. J.; Ritchie, J. P. *J. Phys. Chem.* **1990**, *94*, 148.
(15) Cioslowski, J.; Hamilton, T.; Scuseria, G.; Hess, B. A., Jr.; Hu, J.; Schaad, L. J.; Dupuis, M. *J. Am. Chem. Soc.* **1990**, *112*, 4183.
(16) Cioslowski, J. *J. Am. Chem. Soc.* **1990**, *112*, 6536.
(17) Cioslowski, J.; Fleischmann, E. D. *J. Chem. Phys.* **1991**, *94*, 3730.
(18) Hariharan, P. C.; Pople, J. A. *Theor. Chim. Acta* **1973**, *28*, 213.
(19) GAUSSIAN 88, Frisch, M. J.; Head-Gordon, M.; Schlegel, H. B.; Raghavachari, K.; Binkley, J. S.; Gonzalez, C.; Defrees, D. J.; Fox, D. J.; Whiteside, R. A.; Seeger, R.; Melius, C. F.; Baker, J.; Martin, R. L.; Kahn, L. R.; Stewart, J. J. P.; Fluder, E. M.; Topiol, S.; Pople, J. A.; Gaussian, Inc.: Pittsburgh PA.
(20) Nelson, R. D.; Lide, D. R.; Maryott, A. A. Selected Values of Electric Dipole Moments for Molecules in the Gas Phase. *Natl. Stand. Ref. Data Ser., Natl. Bur. Stand.*, **1967**, No. 10.

Table III. Calculated Properties of Bonds in CHX_3 and CX_3^-[a]

system	bond	r_1[b]	r_2[c]	ρ_{crit}	$\nabla^2\rho_{crit}$	ϵ[d]
CHF_3	C–H	1.3496	0.6802	0.3206	−1.3989	0.0000
		(1.3286)	(0.7011)	(0.3308)	(−1.5037)	(0.0000)
	C–F	0.7930	1.6953	0.2825	0.2978	0.1820
		(0.7935)	(1.6947)	(0.2830)	(0.2753)	(0.1778)
CF_3^-	C–F	0.8366	1.8295	0.2075	0.2976	0.9022
		(0.8405)	(1.8257)	(0.2100)	(0.2257)	(0.7987)
$CH(CN)_3$	C–H	1.3662	0.6847	0.2880	−1.1325	0.0000
		(1.3330)	(0.7180)	(0.2982)	(−1.2144)	(0.0000)
	C–C	1.2958	1.4956	0.2722	−0.8100	0.0344
		(1.2970)	(1.4944)	(0.2721)	(−0.8079)	(0.0329)
	C–N	0.7245	1.4145	0.4896	0.9454	0.0071
		(0.7249)	(1.4140)	(0.4902)	(0.9172)	(0.0077)
$C(CN)_3^-$	C–C	1.1123	1.5565	0.2922	−0.9044	0.4217
		(1.1150)	(1.5538)	(0.2925)	(−0.9057)	(0.4140)
	C–N	0.7347	1.4294	0.4820	0.5002	0.0840
		(0.7351)	(1.4290)	(0.4829)	(0.4741)	(0.0844)
$CH(NO_2)_3$	C–H	1.3867	0.6405	0.3069	−1.3394	0.0000
		(1.3573)	(0.6698)	(0.3187)	(−1.4476)	(0.0000)
	C–N	1.0929	1.7186	0.2815	−0.9914	0.0815
		(1.0840)	(1.7275)	(0.2810)	(−0.9937)	(0.0828)
	$N–O_1$	1.0799	1.1519	0.5635	−1.4383	0.1386
		(1.0806)	(1.1512)	(0.5627)	(−1.4216)	(0.1411)
	$N–O_2$	1.0879	1.1527	0.5579	−1.3995	0.1380
		(1.0844)	(1.1522)	(0.5572)	(−1.3866)	(0.1399)
$C(NO_2)_3^-$	C–N	0.8447	1.8068	0.2994	−0.3579	1.5039
		(0.8432)	(1.8084)	(0.2985)	(−0.3342)	(1.5236)
	$N–O_1$	1.1098	1.1632	0.5370	−1.3041	0.1308
		(1.1101)	(1.1628)	(0.5363)	(−1.2924)	(0.1318)
	$N–O_2$	1.1098	1.1632	0.5370	−1.3041	0.1308
		(1.1101)	(1.1628)	(0.5363)	(−1.2924)	(0.1318)
	$O_1–O_2$	2.5262	2.5262	0.0169	0.0687	0.0931
		(2.5261)	(2.5261)	(0.0167)	(0.0682)	(0.1118)
	$O_1–O_2$ (rp)	2.6077	2.6077	0.0159	0.0912	n/a
		(2.6027)	(2.6027)	(0.0158)	(0.0897)	n/a

[a] At the HF/6-31G* optimized geometries. The HF/6-31++G** values are in parentheses. In the $CH(NO_2)_3$ molecule, the O_1 (O_2) atoms are positioned below (above) the plane containing the nitrogen atoms. The critical points of the C–N–O–O–N rings are listed under $O_1–O_2$ (rp). All entries in au. [b] Distance between the first atom listed and the critical point. [c] Distance between the second atom listed and the critical point. [d] Bond ellipticity.[23]

lengths and stretching force constants. The values of both the C–H bond lengths and the C–H force constants are quite insensitive to the substituents.

The computed geometries of the anions require a special comment. A previous calculation by Edgecombe and Boyd[3] at the STO-3G level yielded a propeller structure with C_3 symmetry for $C(NO_2)_3^-$. Our calculations, however, show that at the HF/6-31G* level, the carbon atom is coplanar with the nitrogens while the oxygens of the nitro groups are rotated out of plane. The result is a structure with D_3 symmetry. The $C(CN)_3^-$ anion is likewise found to be planar, while the CF_3^- ion exhibits a pyramidal geometry. In addition, we observe in $C(CN)_3^-$ a shortening of the carbon–carbon bond and a lengthening of the carbon–nitrogen bond relative to $CH(CN)_3$. We also find an analogous shortening of the carbon–nitrogen bond and lengthening of the nitrogen–oxygen bond in $C(NO_2)_3^-$ relative to $CH(NO_2)_3$. In contrast, the C–F bond length increases upon going from CHF_3 to CF_3^-. The planarity of the $C(NO_2)_3^-$ and $C(CN)_3^-$ ions and the changes in bond lengths are obvious consequences of Y-aromaticity in these systems.[21]

We note that the geometry of $CH(NO_2)_3$ is consistent with that needed to produce the observed rotational spectrum.[22] The spectrum indicates that the molecule is a symmetric top. Moreover, it also features a "peculiar" set of six evenly spaced lines of roughly equal intensities associated with each $J \rightarrow J + 1$ transition. These lines are observed even at low Stark modulating voltages. Caminati and Wilson[22] have carried out a group-theoretical analysis of the possible structures of trinitromethane and have concluded that each NO_2 group should have a small twist angle with respect to the C_{3v} configuration. These NO_2 groups would each contribute a symmetric and an antisymmetric twist

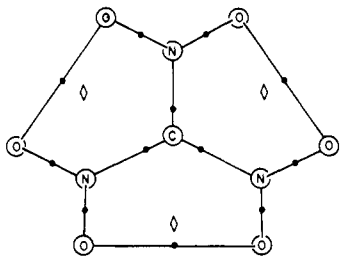

Figure 2. Molecular graph of the $C(NO_2)_3^-$ anion. Heavy dots denote bond points and diamonds denote ring points.

state to yield six torsional levels that are very close in energy.

The results of the topological analysis of the electron densities in the molecules under study are displayed in Table III. Although ρ_{crit} and $\nabla^2\rho_{crit}$ of the C–H bonds appear to be correlated, there is no correlation of either quantity with the distances from the carbon or hydrogen nuclei to the bond critical point. This is true for both the HF/6-31G* and HF/6-31++G** densities. Overall, the computed densities at the critical points are quite insensitive to the augmentation of the basis set with diffuse functions. The indices of the C–H bonds show larger variations with the basis sets, due to the fact that the smaller basis set lacked polarization function on the hydrogen atoms.

Comparison of the electronic densities in cyanoform and nitroform with those of their conjugate bases confirms the presence of Y-aromaticity in the $C(CN)_3^-$ and $C(NO_2)_3^-$ anions. The electron densities at the critical points belonging to the C–C bonds in $CH(CN)_3$ and the C–N bonds in $CH(NO_2)_3$ increase upon deprotonation, whereas the densities of the respective C–N and N–O bonds decrease. This is in agreement with the expected changes in the bond orders due to conjugation effects in anions. The analogous effects are observed in the values of $\nabla^2\rho_{crit}$.

(21) Gund, P. *J. Chem. Educ.* **1972**, *49*, 100.
(22) Caminati, W.; Wilson, E. B. *J. Mol. Spectrosc.* **1980**, *81*, 507.

Table IV. Calculated Bader and GAPT Atomic Charges in CHX_3 and CX_3^-[a]

system	atom	Q_{Bader} 6-31G*	Q_{Bader} 6-31++G**	Q_{GAPT} 6-31G*
CHF_3	H	0.0864	0.0659	−0.0612
	C	2.1478	2.1652	1.7895
	F	−0.7440	−0.7430	−0.5761
CF_3^-	C	1.3985	1.3885	1.1823
	F	−0.7989	−0.7951	−0.7274
$CH(CN)_3$	H	0.1547	0.1167	0.0663
	C	0.4156	0.4533	0.6093
	C_{cyano}	1.2250	1.2256	0.0244
	N	−1.4148	−1.4148	−0.2496
$C(CN)_3^-$	C	0.4029	0.3979	−0.6500
	C_{cyano}	1.1527	1.1529	0.6014
	N	−1.6205	−1.6191	−0.7180
$CH(NO_2)_3$	H	0.2045	0.1725	0.0729
	C	1.0307	1.0679	0.4987
	N	0.5424	0.5297	1.2520
	O_1	−0.4690	−0.4662	−0.6970
	O_2	−0.4871	−0.4869	−0.7456
$C(NO_2)_3^-$	C	1.3379	1.3406	−0.9195
	N	0.3595	0.3558	1.6786
	O_1	−0.5694	−0.5680	−0.8527
	O_2	−0.5694	−0.5680	−0.8527

[a] At the HF/6-31G* optimized geometries. The last digits in the Bader charges may be uncertain. In the $CH(NO_2)_3$ molecule, the O_1 (O_2) atoms are positioned below (above) the plane containing the nitrogen atoms.

The molecular graphs[8] of the systems show no unexpected features except in the case of the trinitromethanide ion. In addition to bond points between nuclei that one would expect to be bonded on the basis of "chemical intuition", the electron density in this ion reveals the existence of three ring points and three additional bond points. These extra bond points correspond to low-ellipticity bonds[23] between oxygen atoms of adjacent nitro groups and are found at both the HF/6-31G* and HF/6-31++G** levels. The molecular graph of this unusual system is shown in Figure 2. In the $CH(NO_2)_3$ molecule, the characteristics of the electron density at the critical points of the two nonequivalent N–O bonds follow the obvious observation that the lengthening of the bond results in a decrease in both ρ_{crit} and the absolute value of $\nabla^2\rho_{crit}$.

Table IV lists the HF/6-31G* and HF/6-31++G** Bader charges together with the HF/6-31G* GAPT charges. A number of trends are evident. First, both Bader and GAPT charges are small for the hydrogens in all the carbon acids. Second, the atomic charge on the carbon atom in CHF_3 is large and positive for both the Bader and the GAPT definitions of atomic charge; this can be attributed to a strong, electron-withdrawing inductive effect of the fluorine substituent. These results are reflected, to a lesser extent, in the carbon charges in CF_3^-.

It is known that the Bader and GAPT charges are sensitive to different features of the electron distribution.[14] This phenomenon is observed in the calculated atomic charges of the cyano and nitro systems. The Bader charges on the carbon atoms are positive for both anions and neutral compounds and remain relatively unchanged upon ionic cleavage of the C–H bond. The respective GAPT charges, on the other hand, have positive values for the neutral compounds and negative values for the anions. It appears that the GAPT charges provide a better representation of the electron distribution in the systems under study, because, as discussed above, bonding in the neutral compounds differs substantially from that in the ionic ones. Taking this into account, one can expect large redistributions of electron densities upon deprotonation. The redistributions are much larger for the GAPT than for the Bader atomic charges. Interestingly, despite the large effect of the diffuse functions set on the calculated total energies, the HF/6-31G* and HF/6-31++G** Bader charges do not differ substantially in anions. In the neutral molecules, the largest differences in charges are found for the hydrogen atoms, which can be explained by the presence of polarization functions on those atoms in the larger basis set. However, the absolute magnitudes of the differences are quite small.

(23) The bond ellipticity, ϵ, is defined as $\epsilon = \lambda_1/\lambda_2 - 1$, where λ_1 and λ_2 are the values of the negative curvatures of the electron density at the bond critical point along the axes perpendicular to the bond path, see ref 9.

Table V. Calculated Absolute Gas-Phase Acidities of CHX_3[a]

X	6-31G*	6-31++G**[b]	6-31++G** + ZPE[c]	exp
F	410.4	393.9	382.9	375.6[d]
CN	313.8	308.9	300.6	n/a
NO_2	321.0	317.2	307.8	n/a

[a] At the HF level. All entries in kcal/mol. [b] At the HF/6-31G* geometries. [c] Zero-point energies calculated from unscaled vibrational frequencies at the HF/6-31G* level. [d] Reference 24.

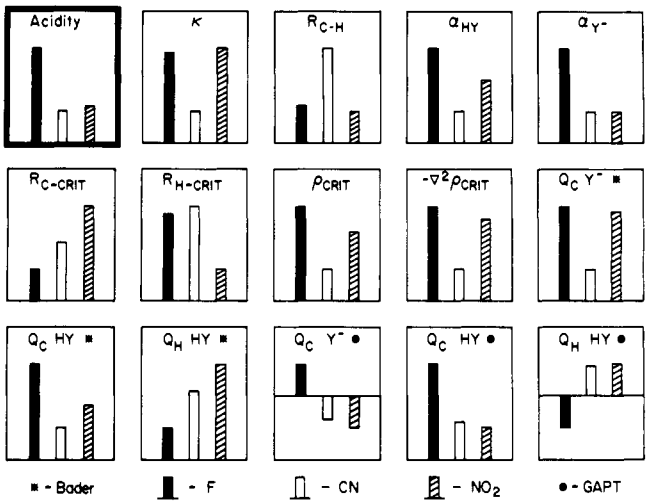

Figure 3. The HF/6-31G* absolute acidities and other electronic properties of the CHX_3 and CX_3^- systems.

We calculated the absolute gas-phase acidities, ΔE, at 0 K as

$$\Delta E = E_{HF}(CX_3^-) - E_{HF}(CHX_3) \quad (1)$$

The results obtained with the 6-31G* and 6-31++G** basis sets, as well as those at the 6-31++G** level including zero-point energy (ZPE), are listed in Table V. The only available experimental value is that for CHF_3,[24] and our best calculated value compares favorably with it. One should also note that the absolute gas-phase acidities calculated with smaller basis sets (3-21G at the STO-3G optimized geometries) and without the ZPE corrections[3] have values consistently larger than the present ones.

Figure 3 shows the attempted correlation of the HF/6-31G* acidities with the following properties calculated at the same level of theory: the C–H bond length, the C–H bond stretching force constant, the angle between the C–X bonds and the C_3 axis for the acid, the corresponding angle between the C–X bonds and the C_3 axis for the conjugate base, the distances from the hydrogen and carbon nuclei to the bond critical point, the electron density at the C–H bond critical point, the Laplacian of the electron density at the C–H bond critical point, and the GAPT and Bader atomic charges on carbon and hydrogen. Although atomic charges have been used successfully to correlate proton affinities as well as other molecular properties for a number of organic compounds,[25-27] we were unable to find a single-parameter correlation of the acidity with any atomic charge or in fact with any of the properties that we studied. The same failure was observed with the HF/6-31++G** properties. One should point out that in the previously reported correlations, the acids and their conjugate bases had similar structures. In our study, however, the geometry of

(24) Bartmess, J. E.; McIver, R. T. In *Gas Phase Ion Chemistry*; Bowers, M. T., Ed.; Academic Press: New York, 1979.
(25) Davis, D. W.; Shirley, D. A. *J. Am. Chem. Soc.* **1976**, *98*, 7898.
(26) Reynolds, W. F.; Mezey, P. G.; Hehre, W. J.; Topsom, R. D.; Taft, R. W. *J. Am. Chem. Soc.* **1977**, *99*, 5821.
(27) French, M. A.; Ikuta, S.; Kebarle, P. *Can. J. Chem.* **1982**, *60*, 1907.

each acid changes radically upon deprotonation.

Conclusions

Ab initio calculations provide a wealth of data on the electronic structure of trisubstituted methanes and their conjugate bases. Properties of the C-H bonds poorly reflect the different origins of the substituent effects in these molecules. On the other hand, the resonance and the inductive effects can be easily distinguished by taking into account large changes in the molecular geometries, the electron densities at the critical points, and the GAPT atomic charges that occur upon deprotonation of the $CH(CN)_3$ and $CH(NO_2)_3$ molecules. The observed trends are in full agreement with the expectations based on the presence of Y-aromaticity in the $C(CN)_3^-$ and $C(NO_2)_3^-$ anions. The GAPT charges appear to provide a better description of the electron density redistribution upon deprotonation than the Bader ones. The changes in molecular geometries are the probable cause of our failure to correlate the proton affinities with either the atomic charges or other molecular parameters. The unusual bonds that are found in the $C(NO_2)_3^-$ anion provide a new challenge to our understanding of chemical bonding.

Acknowledgment. This research was partially supported by the U.S. D.O.E. under contract DE-FC05-85ER250000 and by the Florida State University through time granted on its VAX digital computers. One of the authors (J.C.) also acknowledges support by the Camille and Henry Dreyfus Foundation New Faculty Award Program.

Energy-Distance Relationship in Chemical Bonding. Accurate Calculation of Potential Energy Curves

Andreas A. Zavitsas

Contribution from the Department of Chemistry, Long Island University, University Plaza, Brooklyn, New York 11201. *Received July 16, 1990*

Abstract: A function is proposed for the accurate calculation of potential energy curves of ground-state diatomics. The calculation requires knowledge of the following properties of the species: bond dissociation energy, infrared stretching frequency, equilibrium internuclear distance, electronegativity difference, effective nuclear charges, and masses. Overall, deviations between calculated and reported potentials are within a factor of 2 of the estimated uncertainties of reported RKR points. Calculated potentials are 1 order of magnitude more accurate than those obtainable with previously available methods and are consistently reliable, with no failures detected in the valence region of 50 potentials available to beyond 50% of dissociation. The calculation is applicable to polyatomic molecules.

A method is proposed for the calculation of potential energy curves describing the energy-distance relationship during the making or breaking of chemical bonds between two atoms. The accuracy obtained approaches the limits of uncertainty of available results for ground-state diatomic species. The search for a "universal" potential energy function goes back at least 60 years: Morse,[1] Rydberg,[2] Pöschl and Teller,[3] Linnett,[4] Frost and Musulin,[5] Varshni,[6] and Lippincott,[7] among others, have attempted to formulate a universally applicable function. Such a method should be capable of accurate calculations of potential energy curves in terms of properties of reactants and products, i.e., the two separated atoms and the diatomic species formed.

The potential curve for each diatomic species can be deduced from spectroscopic measurements, involving transitions to various vibrational levels of the particular bond, through the RKR procedure.[2,8,9] This calculation gives the energy of each vibrational level from the bottom of the potential curve and two corresponding distances or "turning points", r_{min} and r_{max}, for each level, thus defining the width of the curve at that energy as shown for H_2 in Figure 1. The energy is for rotational quantum number $J = 0$. The RKR procedure is a semiclassical, first-order method producing potentials within the Born-Oppenheimer approximation. Experimental results are often more accurately described by the method of inverse perturbation analysis (IPA), which is less subject to approximations associated with RKR.[10] RKR and similar procedures are the only relatively direct methods available for establishing distances and corresponding energies in a "reaction coordinate", the reaction being the breaking or making of a chemical bond.

At present, no procedures exist, either semiempirical or ab initio, for the accurate calculation of potential energy curves. Desired accuracies for realistic descriptions generally are average deviations between calculated and RKR energies of less than ±1% of the bond dissociation energy of the species or, alternatively, of less than the "chemical" accuracy of ±1 kcal/mol (349.74 cm^{-1}, 4.184 kJ/mol). Ab initio calculations have produced a very accurate description of the potential energy curve for the ground state of H_2,[11] but such calculations become increasingly less accurate with

(1) (a) Morse, P. M. *Phys. Rev.* **1929**, *34*, 57-64. (b) Rosen, N.; Morse, P. M. *Phys. Rev.* **1932**, 210.
(2) Rydberg, R. *Z. Phys.* **1931**, *73*, 376. *Ibid.* **1933**, *80*, 514.
(3) Pöschl, G.; Teller, E. *Z. Phys.* **1933**, *83*, 143.
(4) Linnett, J. W. *Trans. Faraday Soc.* **1940**, *36*, 1123. *Ibid.* **1942**, *38*, 1.
(5) Frost, A. A.; Musulin, B. *J. Chem. Phys.* **1954**, *22*, 1017; *J. Am. Chem. Soc.* **1954**, *76*, 2045.
(6) Varshni, Y. P. *Rev. Mod. Phys.* **1957**, *29*, 664-682.
(7) (a) Lippincott, E. R. *J. Chem. Phys.* **1953**, *21*, 2070. *Ibid.* **1955**, *23*, 603. (b) Lippincott, E. R.; Schroeder, R. *J. Chem. Phys.* **1955**, *23*, 1099. *Ibid.* **1955**, *23*, 1131; *J. Am. Chem. Soc.* **1956**, *78*, 5171; *J. Phys. Chem.* **1957**, *61*, 921. (c) Lippincott, E. R.; Dayhoff, M. O. *Spectrochim. Acta* **1960**, *16*, 807. (d) Lippincott, E. R. *J. Chem. Phys.* **1957**, *26*, 1678. (e) Lippincott, E. R.; Steele, D.; Caldwell, P. *J. Chem. Phys.* **1961**, *35*, 123. (f) Steele, D.; Lippincott, E. R. *J. Chem. Phys.* **1961**, *35*, 2065-2075.
(8) Klein, O. *Z. Phys.* **1932**, *76*, 226.
(9) Rees, A. L. G. *Proc. Phys. Soc., London, Sect. A* **1947**, *59*, 998.
(10) Kosman, W. M.; Hinze, J. *J. Mol. Spectrosc.* **1975**, *56*, 93-103. Vidal, C. R.; Scheingraber, H. *Ibid.* **1977**, *65*, 46-64.
(11) (a) Kolos, W.; Szalewicz, K.; Monkhorst, H. J. *J. Chem. Phys.* **1986**, *84*, 3278-3283. (b) Kolos, W.; Wolniewicz, L. *J. Chem. Phys.* **1968**, *49*, 404-410. (c) *Ibid.* **1965**, *43*, 2429-2441.

0002-7863/91/1513-4755$02.50/0